Cutting force-based adaptive neuro-fuzzy approach for accurate surface roughness prediction in end milling operation for intelligent machining

Ibrahem Maher, M. E. H. Eltaib, Ahmed A. D. Sarhan & R. M. El-Zahry

The International Journal of Advanced Manufacturing Technology

ISSN 0268-3768
Volume 76
Combined 5-8

Int J Adv Manuf Technol (2015)
76:1459-1467
DOI 10.1007/s00170-014-6379-1

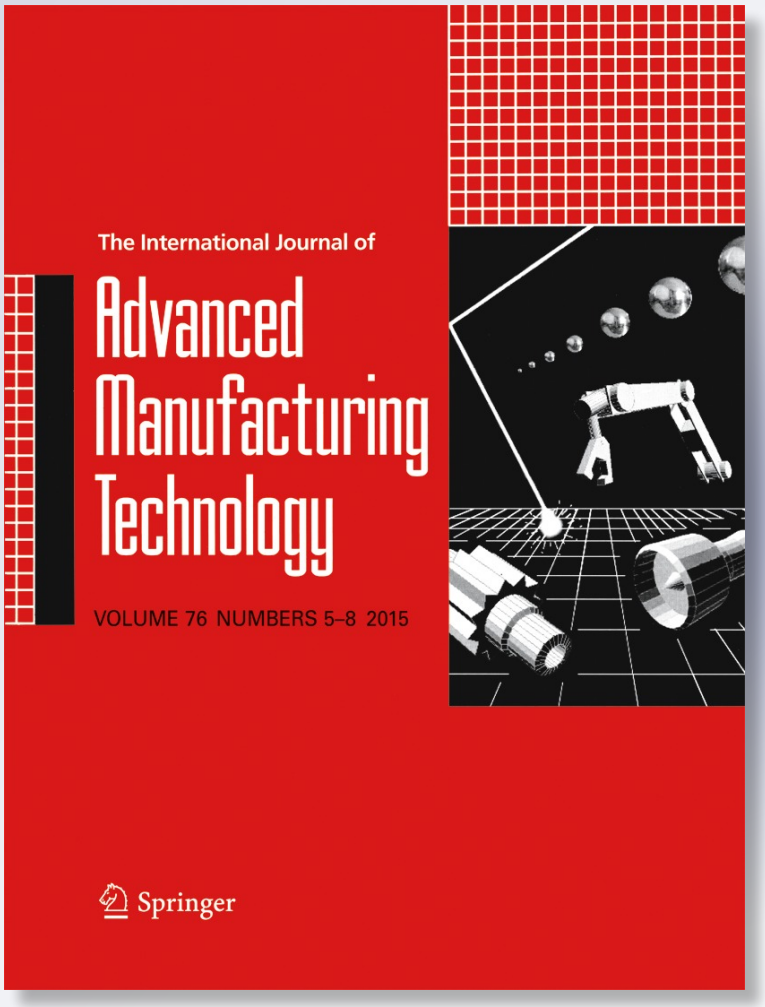

Springer

Int J Adv Manuf Technol (2015) 76:1459–1467
DOI 10.1007/s00170-014-6379-1

ORIGINAL ARTICLE

Cutting force-based adaptive neuro-fuzzy approach for accurate surface roughness prediction in end milling operation for intelligent machining

Ibrahem Maher · M. E. H. Eltaib · Ahmed A. D. Sarhan · R. M. El-Zahry

Received: 9 November 2013 / Accepted: 8 September 2014 / Published online: 19 September 2014

Abstract End milling is one of the most common metal removal operations encountered in industrial processes. Product quality is a critical issue as it plays a vital role in how products perform and is also a factor with great influence on manufacturing cost. Surface roughness usually serves as an indicator of product quality. During cutting, surface roughness measurement is impossible as the cutting tool is engaged with the workpiece, chip and cutting fluid. However, cutting force measurement is easier and could be used as an indirect parameter to predict surface roughness. In this research work, a correlation analysis was initially performed to determine the degree of association between cutting parameters (speed, feed rate, and depth of cut) and cutting force and surface roughness using adaptive neuro-fuzzy inference system (ANFIS) modeling. Furthermore, the cutting force values were employed to develop an ANFIS model for accurate surface roughness prediction in CNC end milling. This model provided good prediction accuracy (96.65 % average accuracy) of surface roughness, indicating that the ANFIS model can accurately predict surface roughness during cutting using the cutting force signal in the intelligent machining process to achieve the required product quality and productivity.

I. Maher (✉) · A. A. D. Sarhan
Centre of Advanced Manufacturing and Material Processing, Department of Mechanical Engineering, University of Malaya, 50603 Kuala Lumpur, Malaysia
e-mail: ibrahemmaher@eng.kfs.edu.eg

I. Maher
Department of Mechanical Engineering, Faculty of Engineering, Kafrelsheikh University, Kafrelsheikh 33516, Egypt

M. E. H. Eltaib · A. A. D. Sarhan · R. M. El-Zahry
Department of Mechanical Engineering, Faculty of Engineering, Assiut University, Assiut 71516, Egypt

Keywords Intelligent machining · End milling · Cutting forces · Surface roughness · CNC · ANFIS

1 Introduction

Machining processes are fundamentally complex, nonlinear, multi variate, and often subjected to various unknown external disturbances. A machining process is usually performed by a skilled operator who uses decision-making capabilities based on the intuition and rules of thumb gained from experience. This process is not accurate enough and in many cases product faults occur. For this reason and to realize highly productive and flexible machining, a reliable, automated machining system with intelligent functions (intelligent machining) is needed [1, 2]. Figure 1 depicts the concept of an intelligent CNC machine. Intelligent NC machine tools have three feedback loop levels for intelligent functions. Among the intelligent functions, cutting force monitoring is an important issues, as it can tell the limits of cutting conditions, workpiece surface quality, and tool wear, as well as detect and prevent tool breakage and chatter, compensate tool deflections, and optimize machining processes through a model-based adaptive control system and other process information, which are indispensable for process feedback control [3–6].

In this research work, cutting force is used to predict surface quality during cutting in an end milling process. Surface quality plays a vital role in milled surfaces by significantly improving fatigue strength, corrosion resistance, and creep life. Moreover, surface quality affects several functional attributes of parts, such as contact causing surface friction, wear, light reflection, heat transmission, ability of distributing and holding lubricant, coating, and resisting fatigue [7, 8].

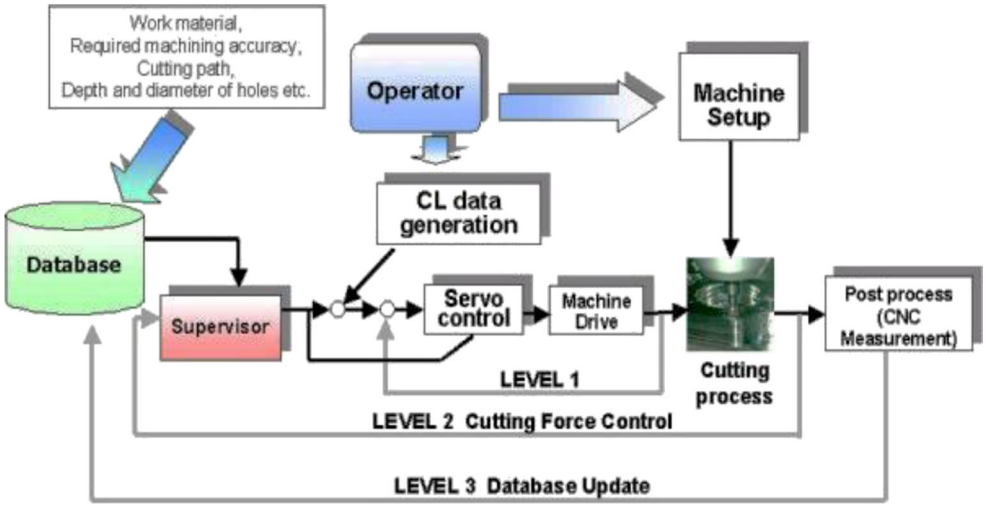

Fig. 1 System configuration of the intelligent NC machine tool [1]

To achieve higher levels of surface quality, correlation modeling of cutting force and surface roughness is required [9–11]. Modeling based on cutting force and surface roughness data is accomplished by soft computing tools [12–14]. Soft computing techniques are useful when exact mathematical information is not available and these differ from conventional computing in that they are tolerant of imprecision, uncertainty, partial truth, approximation, and met heuristics [15, 16]. ANFIS is one of the soft computing techniques that play a significant role in input–output matrix relationship modeling. It is used when subjective knowledge and expert suggestions are significant to defining objective function and decision variables. ANFIS is ideal to predict surface roughness based on input variables due to the nonlinear condition in the machining process [17–21].

As a conclusion of the above review, the aim of the present work is to investigate the use of cutting force-based ANFIS modeling for accurate surface roughness prediction in end milling operation for intelligent machining.

2 Experimental setup

The experimental setup is shown in Fig. 2. The experiments were performed using a CNC end milling machine. A high-speed steel four-flute end milling cutter with a diameter of 7/16 in (11.1 mm) was used for dry machining slots of Brass (60Cu40Zn) blocks under specific machining conditions, as shown in Table 1. These machining conditions were selected based on the tool maker's recommendations. Brass material with Vickers hardness of 125 and chemical composition of 60 % Copper and 40 % Zinc was used as workpiece material with 40×40×20 mm dimensions.

The surface roughness (*Ra*) was measured with a stylus-based profilometer (Surtronic 3+, accuracy of 99 %). The average surface roughness was calculated for three different measurements under the same conditions with a sampling

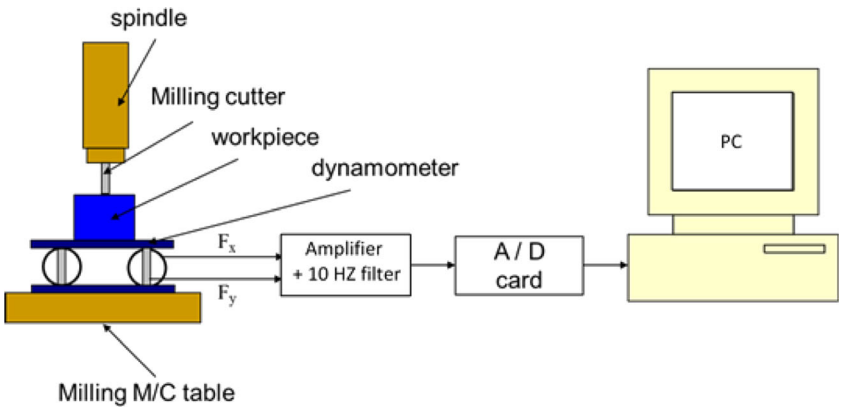

Fig. 2 Experimental setup

Table 1 Cutting parameters levels

Cutting parameters	Unit	Symbol	Level 1	Level 2	Level 3	Level 4	Level 5
Spindle speed	rpm	n	750	1000	1250	1500	1750
Feed rate	mm/min	f	50	100	150	200	250
Depth of cut	mm	t	0.3	0.5	0.7		

length of Lc=2.5 mm at a specific area of the workpiece. The measurements' direction was parallel to the cutting direction and perpendicular to the lay of surface anomalies. On the other hand, the cutting forces were measured using a strain gauge-based analogue dynamometer. The analogue values obtained from the dynamometer were amplified, filtered with 10 Hz low bass filter and recorded on a computer using a 12 bit analogue-to-digital converter.

3 Experimental results and ANFIS modeling

The measured cutting forces and surface roughness shown in Table 2 were used as the training data set to build the ANFIS model. Five network layers were used by ANFIS to perform the following fuzzy inference steps as shown in Fig. 3: layer 1—input fuzzification, layer 2—fuzzy set database construction, layer 3—fuzzy rule base construction, layer 4—decision making, and layer 5—output defuzzification [22–24].

To explain this model simply, two rules and two linguistic values for each input variable are suggested.

Layer 1 The output of the node is the degree to which the given input satisfies the linguistic label associated to this node. Usually, bell-shaped membership functions are chosen to represent the linguistic terms because the relationship between the cutting parameters and surface roughness is not linear (Fig. 4a).

First parameter membership functions

$$A_i(x) = exp\left[-0.5((x-a_{i1})/b_{i1})^2\right] \quad (1)$$

Second parameter membership functions

$$B_i(y) = exp\left[-0.5((y-a_{i2})/b_{i2})^2\right] \quad (2)$$

where a_{i1}, a_{i2}, b_{i1}, and b_{i2} are the parameter set.

As the values of these parameters change, the bell-shaped functions vary accordingly, as shown in Fig. 4b, thus

Table 2 Measured cutting forces and surface roughness (training data set)

n (rpm)		750		1000		1250		1500		1750	
f (mm/min)	t (mm)	F (N)	Ra (μm)	F (N)	Ra (μm)	F (N)	Ra (μm)	F (N)	Ra (μm)	F (N)	Ra (μm)
50	0.3	25.61	1.1	15.26	0.96	10.63	1.18	11.31	0.6	7.21	0.84
	0.5	39.81	1.36	30.53	1.12	14.87	1.6	19.80	0.82	12.04	0.82
	0.7	50.61	1.9	37.54	1.36	22.63	1.08	27.59	1.02	12.73	1.54
100	0.3	33.42	1.28	17.03	1.02	10.82	1.18	14.87	0.86	20.52	0.98
	0.5	64.88	2.06	44.05	1.44	21.21	1.3	30.48	1.02	45.45	1.16
	0.7	106.83	2.22	62.94	1.78	25.50	1.14	40.61	1.24	73.36	1.22
150	0.3	31.14	1.42	21.21	1.54	18.44	1.24	20.52	1.32	31.62	1.1
	0.5	81.84	2.63	50.22	1.54	22.80	1.34	37.01	1.36	70.04	1.26
	0.7	113.81	2.96	78.49	2.24	32.53	1.22	52.40	1.38	92.44	1.62
200	0.3	30.41	1.54	18.38	1.16	22.63	1.26	25.24	1.56	39.56	1.32
	0.5	78.77	3.5	61.62	2.28	30.41	1.5	49.24	1.56	86.56	1.62
	0.7	144.90	3.52	102.53	2.64	42.64	1.44	56.82	1.4	104.24	1.6
250	0.3	70.21	1.82	23.02	1.58	25.50	1.66	35.47	1.32	56.65	1.48
	0.5	58.67	2.5	61.59	2.96	28.32	1.38	54.08	1.26	106.96	1.74
	0.7	190.80	5.5	106.78	3.14	38.18	1.62	49.52	1.42	107.94	1.56

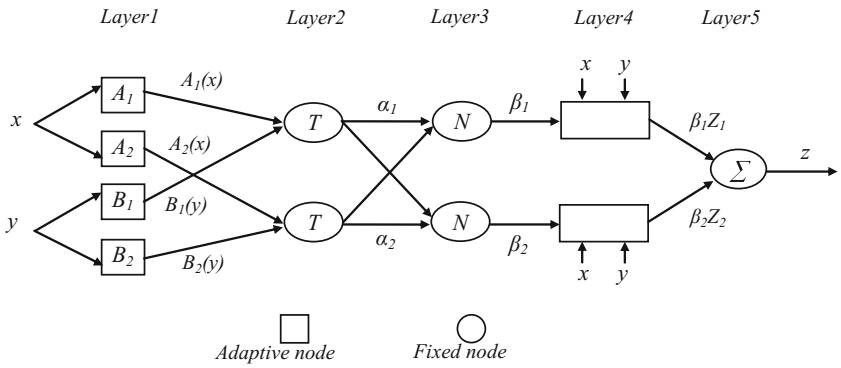

Fig. 3 ANFIS architecture for a two-input Sugeno fuzzy model

exhibiting various forms of membership functions on linguistic labels A_i and B_i. The parameters in this layer are referred to as principle parameters.

Layer 2 Each node computes the firing strength of the associated rule. The nodes of this layer are called rule nodes. The outputs of the top and bottom neurons are as follows:

Top neuron

$$\alpha_1 = A_1(x) \times B_1(y) \tag{3}$$

Bottom neuron

$$\alpha_2 = A_2(x) \times B_2(y) \tag{4}$$

Layer 3 Every node in this layer is labeled by N to indicate the normalization of the firing levels. The output of the top and bottom neurons is normalized as follows:

Top neuron

$$\beta_1 = \alpha_1/(\alpha_1 + \alpha_2) \tag{5}$$

Bottom neuron

$$\beta_2 = \alpha_2/(\alpha_1 + \alpha_2) \tag{6}$$

Layer 4 The output of the top and bottom neurons is the product of the normalized firing level and the individual rule output of the first rule and second rule, respectively.

Top neuron

$$\beta_1 z_1 = \beta_1(a_1 x + b_1 y) \tag{7}$$

Bottom neuron

$$\beta_2 z_2 = \beta_2(a_2 x + b_2 y) \tag{8}$$

Layer 5 The single node in this layer computes the overall system output as the sum of all incoming signals, i.e.,

$$z = \beta_1 z_1 + \beta_2 z_2 \tag{9}$$

If a crisp training set $((x^k, y^k), k=1, \ldots, k)$ is given, then the parameters of the hybrid neural net (which determine the shape of the membership functions of the premises) can be learned by descent-type methods. The error function for pattern k can be given by:

$$E_k = \left(y^k - o^k\right)^2 \tag{10}$$

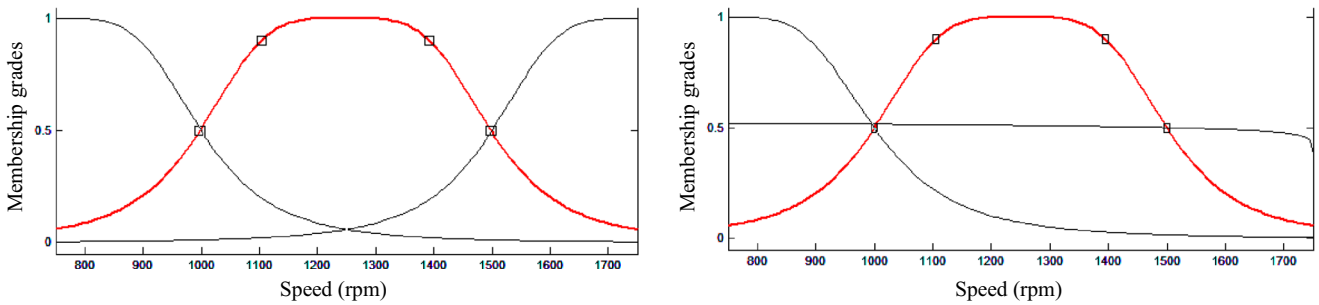

a) Initial membership function of speed **b)** Final membership function of speed

Fig. 4 Initial and final membership function of speed. **a** Initial membership function of speed. **b** Final membership function of speed

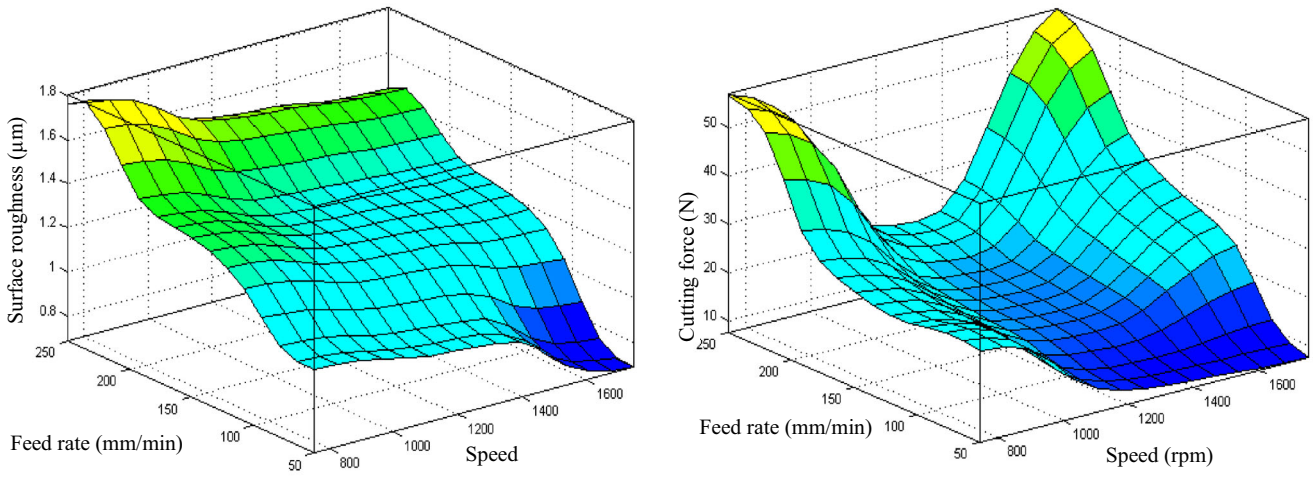

a) Variation of surface roughness with cutting parameters **b)** Variation of cutting force with cutting parameters

Fig. 5 The variation of surface roughness and cutting force with spindle speed and feed rate at 0.3-mm depth of cut. **a** Variation of surface roughness with cutting parameters. **b** Variation of cutting force with cutting parameters

where y^k is the desired output and o^k is the computed output by the hybrid neural net [24].

4 ANFIS prediction model results and discussion

Figures 5, 6, 7, and 8 show the effects of the machining parameters on surface roughness and cutting force. In Fig. 5 at low depth of cut level (0.3 mm), it can be seen that the surface roughness decreases with increasing spindle speed and decreasing feed rate (Fig. 5a). This is because surface roughness is defined as the machining marks on the workpiece surface related to the geometry of the tool edge (Fig. 6 and Eq. 11) which is proportional to the feed rate [25, 26].

$$Ra = \frac{f_z^2}{t_r 18\sqrt{3}} \quad (f_z \leq 2t_r sin(\psi)) \tag{11}$$

Figure 5b shows that the resultant cutting force decreases with increasing rotational speed at a low feed rate range (50 to 100 mm/min) for all ranges of cutting speed. But at feed rate ranging from 100 to 250 mm/min, the cutting force decreases with increasing rotational speed for speed ranging from 750 to 1350 rpm and then the cutting force increases with increasing rotational speed for speed ranging from 1350 to 1750 rpm. This is mainly attributed to built-up edge formed at low speed, where the chip parts become a stationary body of highly deformed material attached to the cutting edge. The growth and rapid breakage of the built-up edge cause a rough surface on the machined part [27–29].

At medium and high depth of cut levels from 0.5 to 0.7 mm and feed rate ranging from 50 to 100 mm/min, the surface roughness and cutting force decrease with increasing rotational speed for all cutting speed ranges. At feed rate ranging from 100 to 250 mm/min, the surface roughness and cutting force decrease with increasing rotational speed for speed ranging from 750 to 1350 rpm; then the surface roughness and cutting force increase with increasing rotational speed for speed ranging from 1350 to 1750 rpm as shown in Figs. 7 and 8.

From the above analysis, it can be seen that the cutting parameters against the cutting force show the same trend as the relations between cutting parameters and surface roughness. This has led to the conclusion that there is a strong correlation between the surface roughness and cutting force. Hence, it is possible to predict the curve trend of surface roughness from the cutting force.

Figure 9 shows the correlation between the cutting force and surface roughness. This figure indicates that surface roughness increases with increasing cutting force and vice versa. It is also clear that the trend of surface roughness change is steady at low cutting force ranging from 7 to 120 N. However, for cutting ranges of more than 120 N, surface roughness rapidly changes.

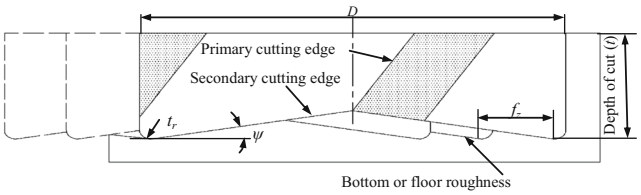

Fig. 6 Geometry of the tool edge in an end-milling

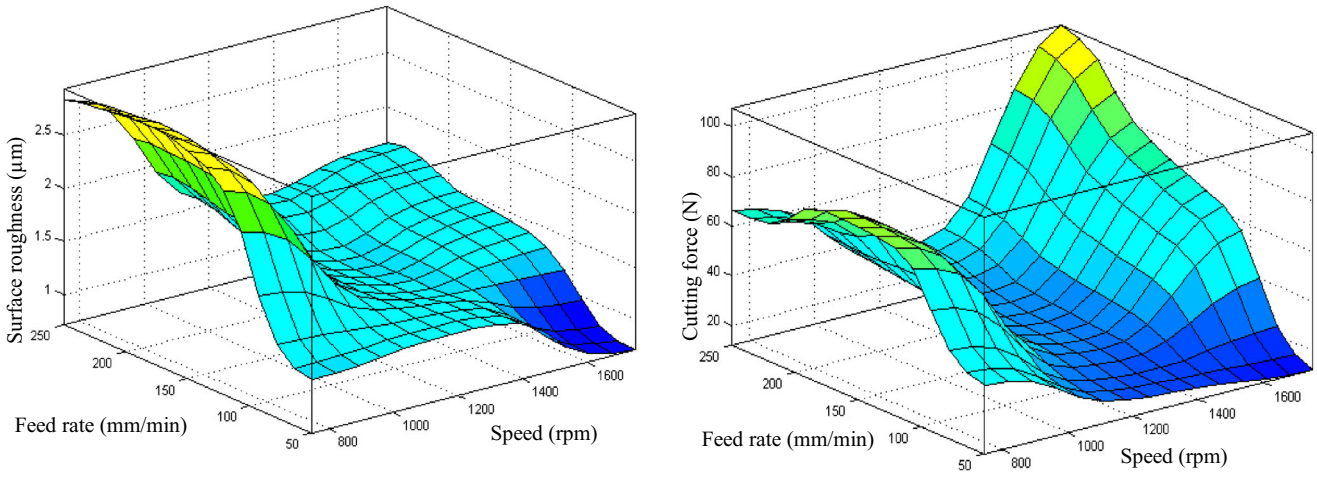

a) Variation of surface roughness with cutting parameters **b)** Variation of cutting force with cutting parameters

Fig. 7 The variation of surface roughness and cutting force with spindle speed and feed rate at 0.5-mm depth of cut. **a** Variation of surface roughness with cutting parameters. **b** Variation of cutting force with cutting parameters

5 ANFIS model verification

Thirty-two random experiments were additionally carried out under different machining conditions for model verification (Table 3). The measured and predicted surface roughness values are also summarized in Table 3. The plot of measured and predicted surface roughness using the ANFIS model is shown in Fig. 10. Appropriate assent is evident between the measured and ANFIS-predicted surface roughness values. This close assent obviously displays that the ANFIS model can be used to predict surface roughness with good conformity. Thus, the proposed ANFIS model offers a promising solution to predicting roughness values in the specific range of parameters.

In addition, Fig. 10 shows high surface roughness at low and high levels of spindle speed (875 and 1625 rpm) and small surface roughness values at medium levels of spindle speed (1125 and 1376 rpm). There is also a big difference in surface roughness between low levels of feed rate (75 to 125 mm/min) and high levels of feed rate (175 to 225 mm/min). Thus, it is recommended to machine brass (60/40) materials using low levels of feed rate (75 to 125 mm/min), medium levels of spindle speed (1125 to 1375 rpm), and small depth of cut levels.

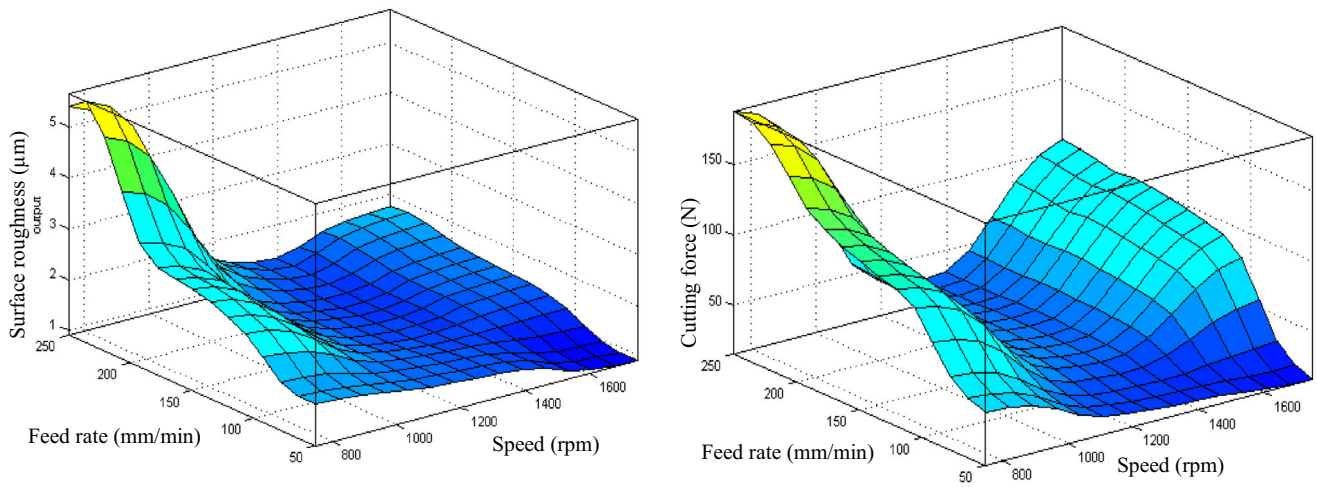

a) Variation of surface roughness with cutting parameters **b)** Variation of cutting force with cutting parameters

Fig. 8 The variation of surface roughness and cutting force with spindle speed and feed rate at 0.7-mm depth of cut. **a** Variation of surface roughness with cutting parameters. **b** Variation of cutting force with cutting parameters

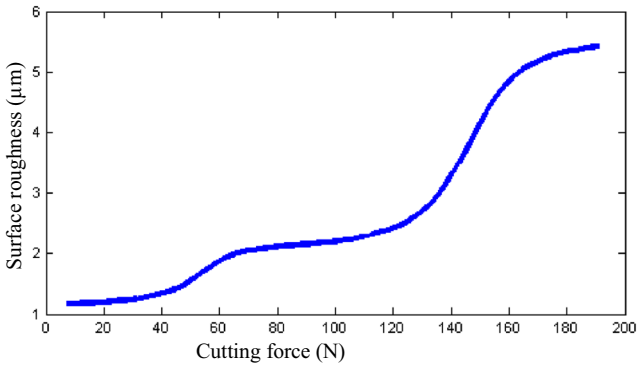

Fig. 9 The variation of surface roughness with cutting force

To investigate the ANFIS model prediction error, the error percentage *Ei* and average error percentage *Eav* are calculated using Eqs. (11) and (12), respectively, and are summarized in Table 3.

$$E_i = \frac{\left|Ra_i - \widehat{Ra}_i\right|}{Ra_i} \times 100 \tag{11}$$

$$E_{av} = \frac{1}{m}\sum_{i=1}^{m} E_i \tag{12}$$

Table 3 Comparison of measured and predicted surface roughness (Ra)

Test no.	Parameters				Measured Ra (μm)	Predicted Ra (μm)	Error E_i (%)	Accuracy (%)
	n (rpm)	*f* (mm/min)	*t* (mm)	*F* (N)				
1	875	75	0.4	43.86	1.42	1.4	1.41	98.59
2			0.6	77.10	2	2.1	5.00	95.00
3		125	0.4	72.35	1.96	2.07	5.61	94.39
4			0.6	98.98	2.36	2.2	6.78	93.22
5		175	0.4	81.06	2.25	2.12	5.78	94.22
6			0.6	126.57	2.66	2.58	3.01	96.99
7		225	0.4	107.17	2.36	2.26	4.24	95.76
8			0.6	125.61	2.61	2.55	2.30	97.70
9	1125	75	0.4	22.02	1.22	1.21	0.82	99.18
10			0.6	36.36	1.36	1.3	4.41	95.59
11		125	0.4	40.00	1.28	1.34	4.69	95.31
12			0.6	66.71	1.89	2.01	6.35	93.65
13		175	0.4	47.71	1.45	1.48	2.07	97.93
14			0.6	69.31	1.92	2.04	6.25	93.75
15		225	0.4	42.94	1.4	1.38	1.43	98.57
16			0.6	62.23	1.96	1.93	1.53	98.47
17	1375	75	0.4	20.62	1.19	1.2	0.84	99.16
18			0.6	23.35	1.18	1.21	2.54	97.46
19		125	0.4	23.60	1.14	1.21	6.14	93.86
20			0.6	32.80	1.33	1.26	5.26	94.74
21		175	0.4	22.02	1.22	1.21	0.82	99.18
22			0.6	33.97	1.32	1.27	3.79	96.21
23		225	0.4	34.06	1.29	1.27	1.55	98.45
24			0.6	39.41	1.32	1.33	0.76	99.24
25	1625	75	0.4	26.08	1.21	1.22	0.83	99.17
26			0.6	40.82	1.3	1.35	3.85	96.15
27		125	0.4	45.18	1.35	1.42	5.19	94.81
28			0.6	65.95	1.91	2	4.71	95.29
29		175	0.4	42.95	1.33	1.38	3.76	96.24
30			0.6	80.80	2.15	2.12	1.40	98.60
31		225	0.4	64.41	1.99	1.97	1.01	98.99
32			0.6	107.62	2.33	2.26	3.00	97.00
Average %							3.35	96.65

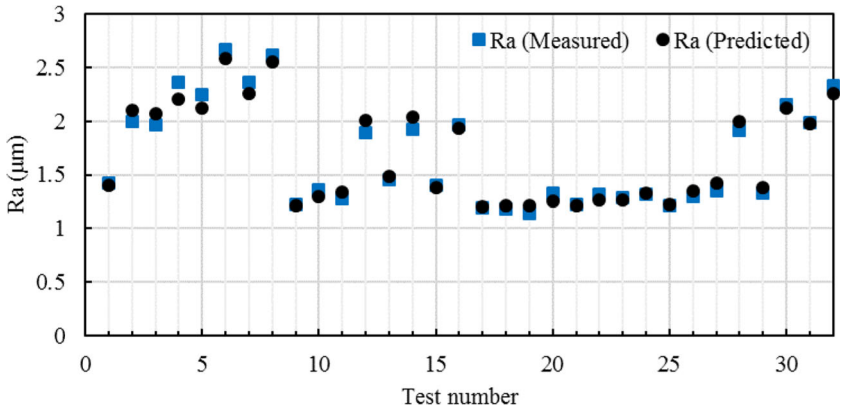

Fig. 10 Measured versus predicted surface roughness (Ra)

where E_i is the percentage error of sample number i, Ra_i is the measured surface roughness of sample number i, $\widehat{Ra}_i$ is the predicted surface roughness generated by the ANFIS model, i=1,2,3,…; m is the sample number, and E_{av} is the average percentage error of m sample data.

Figure 11 indicates that the average percentage error for surface roughness prediction is 3.35 % (96.65 % accuracy). It is also shown that the highest percentage of error for ANFIS model prediction is 6.78 %. The low error level signifies that the surface roughness results predicted by ANFIS are very close to the actual experimental results. The low error and high accuracy levels mean that the proposed model can predict surface roughness satisfactorily.

6 Conclusion

In this research work, a cutting force-based adaptive neuro-fuzzy approach for accurate surface roughness prediction during cutting was established. First, 75 measured surface roughness (*Ra*) and cutting force (*F*) values under different cutting conditions were used as the training data set to build the ANFIS model. The variations in surface roughness and cutting force with the machining parameters (spindle speed, feed rate, and depth of cut) were established. Second, a correlation analysis was performed to determine the degree of association between the cutting parameters with cutting force and surface roughness. Finally, the model was verified using a 32 testing data set, and the average percentage accuracy achieved was 96.65 %, indicating that it is possible to predict surface roughness using an indirect cutting force measurement based on the ANFIS model.

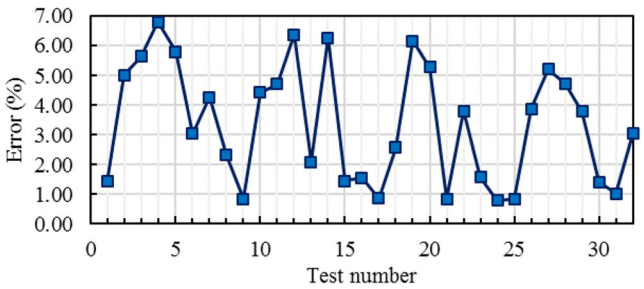

Fig. 11 The error percentage

References

1. Sánchez JA, Ortega N (2009) Machine tools for high performance machining. Machine Tools for High Performance Machining. Springer London. doi:10.1007/978-1-84800-380-4_9
2. Ramesh R, Ravi Kumar KS, Anil G (2009) Automated intelligent manufacturing system for surface finish control in CNC milling using support vector machines. Int J Adv Manuf Technol 42(11–12):1103–1117. doi:10.1007/s00170-008-1676-1
3. Hamdan A, Sarhan AAD, Hamdi M (2012) An optimization method of the machining parameters in high-speed machining of stainless steel using coated carbide tool for best surface finish. Int J Adv Manuf Technol 58(1–4):81–91. doi:10.1007/s00170-011-3392-5
4. Sayuti M, Sarhan AAD, Tanaka T, Hamdi M, Saito Y (2013) Cutting force reduction and surface quality improvement in machining of aerospace duralumin AL-2017-T4 using carbon onion nanolubrication system. Int J Adv Manuf Technol 65(9–12):1493–1500. doi:10.1007/s00170-012-4273-2
5. Davim JP (2008) Machining : fundamentals and recent advances. springer, British Library Cataloguing in Publication Data. doi:10.1007/978-1-84800-213-5
6. Yang L-D, Chen JC, Chow H-M, Lin C-T (2005) Fuzzy-nets-based in-process surface roughness adaptive control system in end-milling operations. Int J Adv Manuf Technol 28(3–4):236–248. doi:10.1007/s00170-004-2361-7
7. Maher I, Eltaib MEH, El-Zahry RM Surface roughness prediction in end milling using multiple regression and adaptive neuro-fuzzy inference system. In: international conference on mechanical engineering advanced technology for industrial production, Assiut University, Egypt, 12-14/December 2006. Assiut University, pp 614–620
8. Asiltürk İ (2012) Predicting surface roughness of hardened AISI 1040 based on cutting parameters using neural networks and multiple regression. Int J Adv Manuf Technol 63(1–4):249–257. doi:10.1007/s00170-012-3903-z
9. Zhang JZ, Chen JC (2006) The development of an in-process surface roughness adaptive control system in end milling operations. Int J

Adv Manuf Technol 31(9–10):877–887. doi:10.1007/s00170-005-0262-z
10. Wang X, Feng C (2002) Development of empirical models for surface roughness prediction in finish turning. Int J Adv Manuf Technol 20(5):348–356
11. Abellan-Nebot J, Romero Subirón F (2010) A review of machining monitoring systems based on artificial intelligence process models. Int J Adv Manuf Technol 47(1–4):237–257. doi:10.1007/s00170-009-2191-8
12. Özel T, Karpat Y (2005) Predictive modeling of surface roughness and tool wear in hard turning using regression and neural networks. Int J Mach Tools Manuf 45(4–5):467–479. doi:10.1016/j.ijmachtools.2004.09.007
13. Sayuti M, Sarhan AAD, Fadzil M, Hamdi M (2012) Enhancement and verification of a machined surface quality for glass milling operation using CBN grinding tool—Taguchi approach. Int J Adv Manuf Technol 60(9–12):939–950. doi:10.1007/s00170-011-3657-z
14. Chandrasekaran M, Muralidhar M, Krishna CM, Dixit US (2010) Application of soft computing techniques in machining performance prediction and optimization: a literature review. Int J Adv Manuf Technol 46(5–8):445–464. doi:10.1007/s00170-009-2104-x
15. Szecsi T (1999) Cutting force modeling using artificial neural networks. J Mater Process Technol 92–93(0):344–349. doi:10.1016/S0924-0136(99)00183-1
16. Zalnezhad E, Sarhan AAD, Hamdi M (2013) A fuzzy logic based model to predict surface hardness of thin film TiN coating on aerospace AL7075-T6 alloy. Int J Adv Manuf Technol 68(1–4):415–423. doi:10.1007/s00170-013-4738-y
17. Kumanan S, Jesuthanam CP, Ashok Kumar R (2008) Application of multiple regression and adaptive neuro fuzzy inference system for the prediction of surface roughness. Int J Adv Manuf Technol 35(7–8):778–788. doi:10.1007/s00170-006-0755-4
18. Chang C-K, Lu HS (2006) Study on the prediction model of surface roughness for side milling operations. Int J Adv Manuf Technol 29(9–10):867–878. doi:10.1007/s00170-005-2604-2
19. Kirby ED, Chen JC, Zhang JZ (2006) Development of a fuzzy-nets-based in-process surface roughness adaptive control system in turning operations. Expert Systems with Applications 30(4):592–604. doi:10.1016/j.eswa.2005.07.005
20. Upadhyay V, Jain PK, Mehta NK (2013) In-process prediction of surface roughness in turning of Ti–6Al–4V alloy using cutting parameters and vibration signals. Measurement 46(1):154–160. doi:10.1016/j.measurement.2012.06.002
21. Maher I, Eltaib MEH, Sarhan AD, El-Zahry RM (2014) Investigation of the effect of machining parameters on the surface quality of machined brass (60/40) in CNC end milling—ANFIS modeling. Int J Adv Manuf Technol:1–7. doi:10.1007/s00170-014-6016-z
22. Kasabov NK (1997) Foundations of neural networks, fuzzy systems, and knowledge engineering, vol 33. Computers & Mathematics with Applications, vol 7. MIT Press, Cambridge, MA. doi:10.1016/S0898-1221(97)84600-7
23. Jang J-SR, Sun C-T, Mizutani E (1997) Neuro-fuzzy and soft computing : a computational approach to learning and machine intelligence. MATLAB curriculum series. Prentice Hall, Inc, USA
24. Fuller R (1995) Neural fuzzy systems. Berlin/Heildelberg,
25. Bhattacharyya A (1996) Metal cutting theory and practice, 1st edn. Agency, New Central Book
26. Childs T, Maekawa K, Obikawa T, Yamane Y (2000) Metal Machining Theory and Applications. John Wiley & Sons Inc, North, Central and South America
27. Philip PK (1971) Built-up edge phenomenon in machining steel with carbide. Int J Mach Tool Des Res 11(2):121–132. doi:10.1016/0020-7357(71)90021-7
28. Fang N, Pai PS, Mosquea S (2010) The effect of built-up edge on the cutting vibrations in machining 2024-T351 aluminum alloy. Int J Adv Manuf Technol 49(1–4):63–71. doi:10.1007/s00170-009-2394-z
29. Cassier Z, Prato Y, Muñoz-Escalona P (2004) Built-up edge effect on tool wear when turning steels at low cutting speed. J Mater Eng Perform 13(5):542–547. doi:10.1361/10599490420629